Research Article

Mechanism of heat-induced damping attenuation for Fe-added Mn–Cu–Al alloys

Yonggang Xu[1,2] · Jin-liu Li[1] · Song Zhang[1]

Received: 24 April 2020 / Accepted: 19 October 2020 / Published online: 18 November 2020

Abstract
The thermotolerance is of great importance for Mn–Cu damping alloys. However, the excessive relaxation behavior of spinodal face-centered cubic (FCC) phases in some thermal environments weakens the kinetics of phase transition from face-centered cubic phase to face-centered tetragonal (FCT) phase, and consequently lower the damping capacity of the alloys. The composition of Fe is regarded as a stabilizing element for FCC phases, but little is known about the role of Fe on the relaxation performance of FCC phases at higher temperatures. The phase structure of the Mn–Cu–Al and Mn–Cu-Al–Fe alloys was analyzed using X-ray diffraction. And their precipitates were observed by using a scanning electron microscopy (SEM) and transmission electron microscope (TEM). Our results show that the excessive relaxation performance happens after holding from 128 to 256 h at 120 ℃. As a result, the amount of FCT phases are decreased and the internal friction has a distinct drop in the meantime. On the other hand, to some extent, the addition of Fe restrains the excessive relaxation performance of the FCC phases. The findings may be helpful for elucidating the mechanism of the heat-induced damping attenuation and promoting the industrial applications of the Mn–Cu alloys.

Keywords Mn–Cu–Al–Fe alloy · Heat-induced damping attenuation · FCC phase · Relaxation performance · FCC–FCT transition

1 Introduction

Since the 1940s, high damping Mn–Cu-based alloys have been well-known because they can damp out the structural or instrumental vibrations [2]. To achieve a higher damping capacity, Deng and Sun et al. reported that the alloys must undergo spinodal decomposition transformation by appropriate heat treatment [1, 8]. A large quantity of nano-twins emerge as a result of an antiferromagnetic transition and a FCC–FCT transition in the spinodal Mn-rich regions. The vibration energy can be dissipated through the boundaries of phases and twins.

However, the Mn-rich FCC phases in Mn–Cu alloys are unstable and may relax after holding at a higher temperature for a long time [2, 3]. Hence, the damping capacity obviously decreases after the thermal holding over the FCT–FCC point. Alloying is often regarded as an efficient method to improve the phase stability. Laddha et al. mentioned that the element of Fe, as an alloying element, affects the FCC phase stability and the phase transition kinetics in Mn–Cu alloys [4]. Furtherly, Sakaguchi et. al reported [7] that the FCC phases in a MnCuNiFe alloy are stabilized by the alloying Fe element. However, little is known about the role of Fe on the stability of spinodal Mn-rich phases and if it affects the damping attenuation of the Mn–Cu alloys.

The aim of this paper is to make clear the effect of Fe on the excessive relaxation of the spinodal FCC phases

✉ Yonggang Xu, yonggang2002@163.com | [1]Key Laboratory for Advanced Technologies of Materials, The Ministry of Education of China, Southwest Jiao Tong University, Chengdu 610031, Sichuan Province, People's Republic of China. [2]Jiangsu Keda Carindustry Co., LTD, Baoyin County, Yangzhou 225800, Jiangsu Province, People's Republic of China.

undergoing a thermal holding above the A_s temperature. In this study, we used the characteristic relaxation time τ as a factor to examine the role of Fe on the stability of Mn-rich FCC phases. The phase structures and precipitations were analyzed using XRD and TEM. The mechanical spectra of the specimens and the FCT–FCC transformation performance were also measured by an inverted torsion pendulum. These investigations provide insights into the mechanism of heat-induced damping attenuation behavior and will be helpful for promoting the thermotolerance of the Mn–Cu alloys.

2 Experimental procedure

2.1 Material preparation

The alloys were prepared from pure electrolytic manganese (> 99.9%), a pure Cu block (> 99.9%), a pure Fe block(> 99.9%), and a pure Al block (> 99.9%) by induction melting in an argon atmosphere (> 99.999%). Table 1 lists the nominal composition of the alloys. Afterward, the as-cast ingots were homogenized at 800 °C for 24 h and air-cooled. At last, the ingots were hot-forged to 15 mm in thickness.

Bulk specimens with the dimensions of 10 mm × 10 mm × 80 mm were spark cut from the 1# and 2# forged sheets. In an electric resistance furnace (SX2-10–13), the bulk specimens were solution-treated at 840 °C for 30 min, and then water-quenched. After that, to achieve a higher damping capacity, the specimens were aged at 430 °C for 60 min and 460 °C for 120 min, respectively.

2.2 Phase transition characteristics and damping performance

To determine the phase transformation point, we measured the mechanical spectrum at forced vibration mode using an inverted torsion pendulum device. The vibration frequency is 1 Hz. The size of the experimental specimens is 1 mm in diameter and 100 mm in length. Their Young's modulus was measured simultaneously as a function of temperature from 25 to 225 °C

To evaluate the effect of thermal storage on the damping capacity, we spark cut two wire specimens of Φ 1.5 × 80 mm from the bulk specimens which had been held in a bath of dimethyl silicone oil at 120 °C at 0, 16, 128, 256, and 512 h, respectively. (The reason will be given in Sect. 3.1) At every abovementioned time point, we measured the internal friction (IF) of the two specimens at room temperature. The range of strain amplitude for IF is from 0×10^{-6} to 1000×10^{-6}, and the vibration frequency is

Table 1 Nominal compositions of the alloys, wt%

	Alloys	Mn	Cu	Al	Fe	Others
1#	Mn–Cu–Al	50.35	45.1	1.55	–	Bal
2#	Mn–Cu–Al–Fe	50.35	43.6	1.55	1.5	Bal

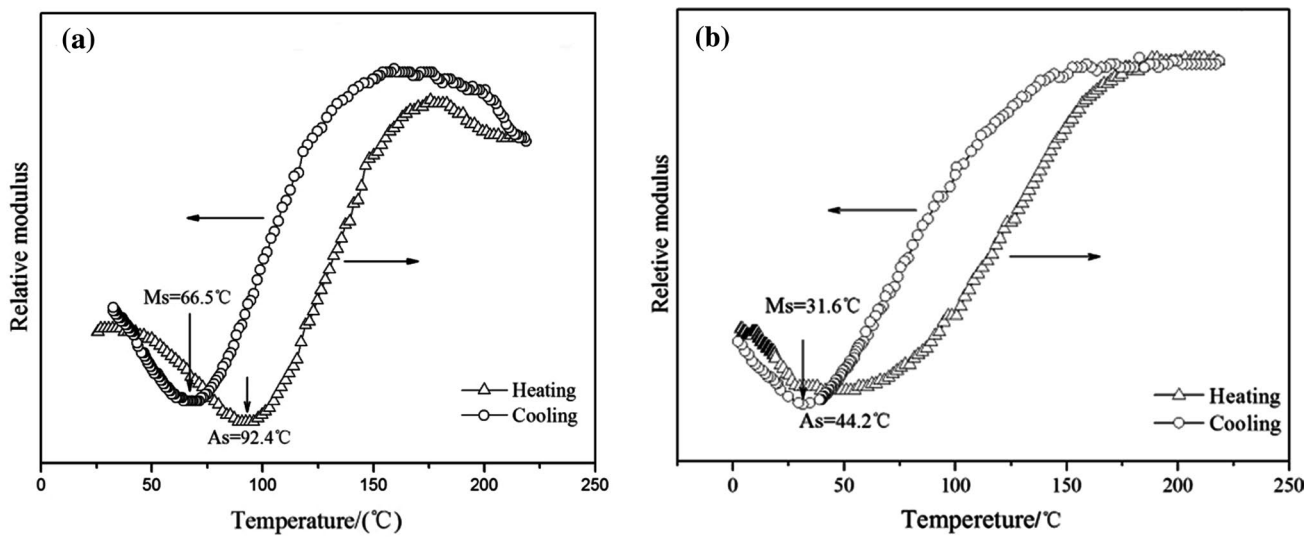

Fig. 1 Mechanical spectroscopies of the alloys. **a** the 1# alloy, between 25 ℃ and 225 ℃. **b** The 2# alloy, between 0 ℃ and 225 ℃

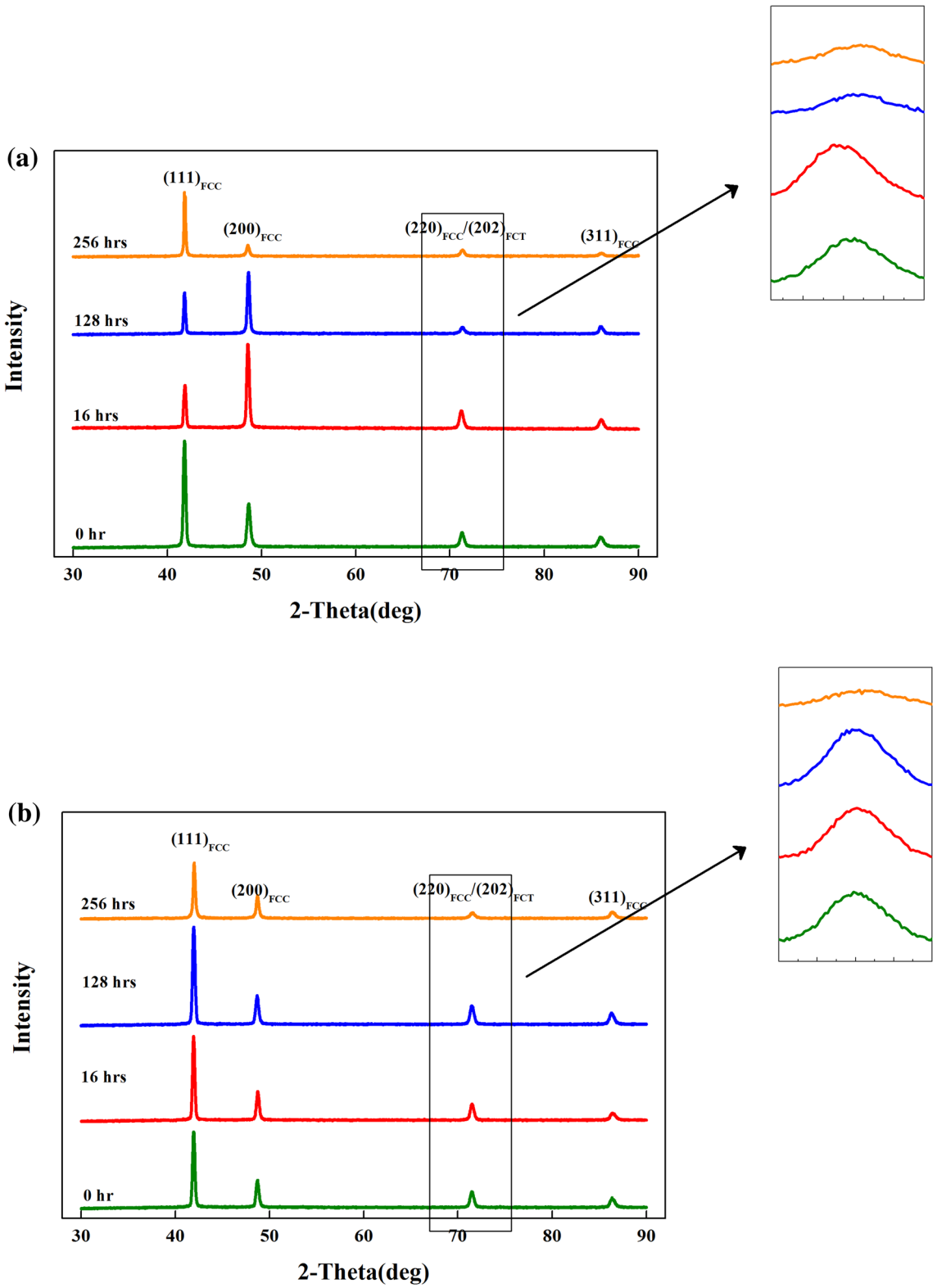

Fig. 2 XRD patterns of the alloys held at 120 °C for different times. **a** The 1# alloy. **b** The 2# alloy

1 Hz. In our experiment, we take the *IF* value at the strain amplitude of 800×10^{-6} as the damping capacity of these specimens.

According to Sakaguchi et al. [7], the degradation kinetics of damping capacity of the alloys can be present as a function of the holding time,

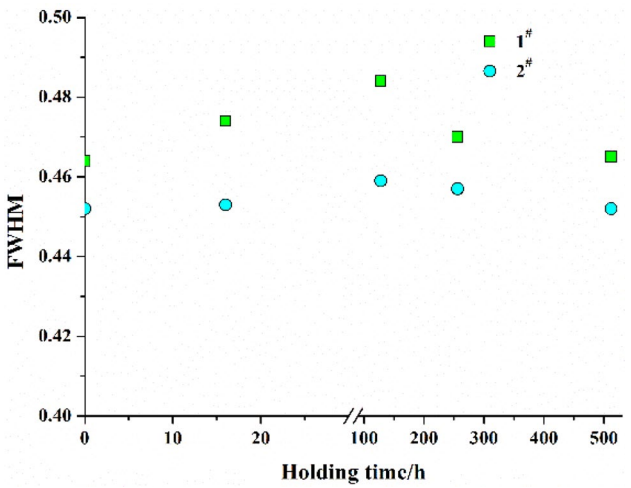

Fig. 3 FWHM values of (220) diffraction peaks for the 1# alloy and 2# alloy held at 120 ℃ for different times

$$\tan\delta = \tan\delta_0 + \tan\delta_D \cdot \exp(-\frac{t}{\tau}) \quad (1)$$

In Eq. (1), $\tan\delta_0$ is the residual damping capacity after holding at 120 °C, $\tan\delta_D$ the amplitude of damping loss due to the instable FCC phases [7], τ the characteristic relaxation time, and t the holding time.

2.3 Microstructural characterization

With Cu K_α radiation and electron diffraction operated at 40 kV and 400 mA, we also examined the diffraction profiles of 110, 200, 220 and 311 of the specimens using a X-ray diffractometer (XRD, X. pert Pro-MPD). All the diffraction profiles were obtained in continuous mode at the scan speed of 0.2°/min.

We examined the microstructure and precipitates of the XRD specimens using scanning electron microscopy (SEM, JS7001). These microstructure analyses were operated at 15 kV acceleration voltage.

To observe the precipitations under TEM, we obtained the discs of 400 μm in thickness by spark cutting the 1# and 2# specimens, and then grinded them to the thickness of 60 μm. After that, the specimens were dimpled and ion milled on Gatan 691 ion milling instrument. Finally, the features of precipitates and their diffraction patterns were examined by using a TEM (Tecnai G2 F20 S-TWIN) operated at 200 kV.

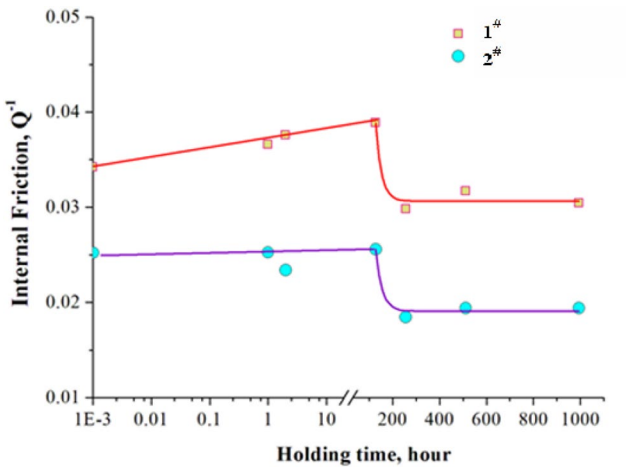

Fig. 4 Damping capacity of the 1# and 2# alloys after holding at 120 ℃ from 0 to 512 h

3 Experimental results

3.1 Phase transition characteristics

Figure 1 shows the mechanical spectrums of the 1# and 2# specimens. We observe a softening performance of Young's modulus, which represent the austenitic and martensitic transitions [6], as the specimens are heated or cooled at the temperature range between 25 and 225 °C. Comparing the curves in Fig. 1a and b, the A_s temperatures of the 1# and 2# specimens are around 92.4 °C and 44.2 °C, respectively. Their Ms temperatures are around 66.5 °C and 31.6 °C, respectively. Conclusively, the phase transition points in the 1# specimen are lowered than those of the 2# specimen, suggesting that the Fe atoms actually lower the A_s and M_s points of the Mn–Cu–Al alloys. Based on the experimental results, we held the specimens at the temperature of 120 °C to examine the relaxation performance of FCC phases.

3.2 XRD

To evaluate the thermal effect on the FCC–FCT transition, we observed their phase structures at room temperature using X-ray diffraction way after holding the 1# and 2# specimens at the temperature of 120℃ for different times. The diffraction profiles of the 1# and 2# specimens are shown in Fig. 2. Unlike high-manganese Mn–Cu alloys [1],

Table 2 Fitting parameters of the damping decrement from 128 to 256 h in Fig. 4

Alloys	Parameters		
	$\tan\delta_0$	$\tan\delta_D$	τ
1#	0.03062	1.43999	24.7869
2#	0.01908	0.74708	26.9677

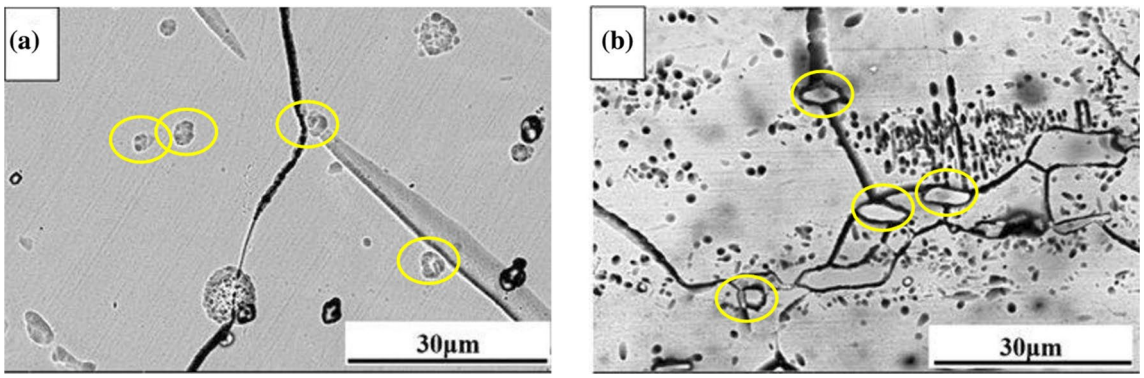

Fig. 5 BSE images of the 1# (**a**) and 2# (**b**) alloys

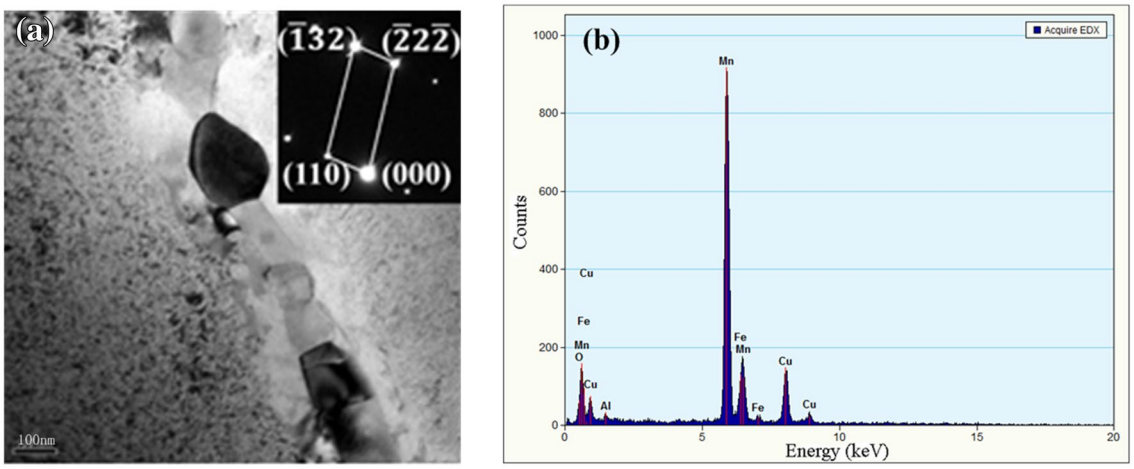

Fig. 6 *α-Mn* phases precipitating in the 1# and 2# alloys. **a** TEM image of the α-*Mn* phases. The inset is the diffraction patterns. **b** EDS spectra of the α-*Mn* phases

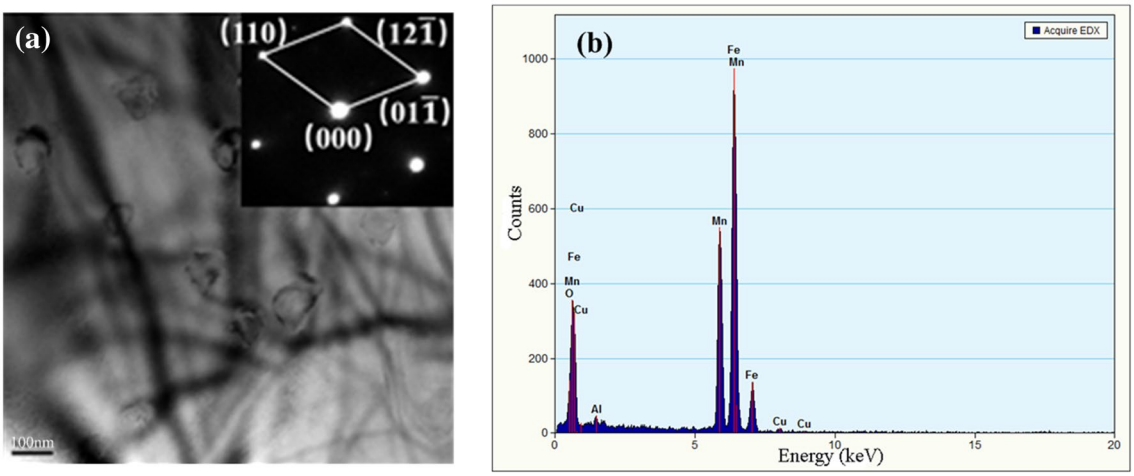

Fig. 7 Fe-rich phases in the 2# alloy. **a** TEM images of the Fe-rich phases. The inset is the diffraction patterns of the Fe-rich phases. **b** EDS spectra for the Fe-rich phases

the (220) peak in Fig. 2 is widened because of the combination of the (220) peak of FCC phases and the (202) peak of FCT phases [5]. Herein, we introduce the full width value at half maximum (FWHM) to estimate the FCT phases in the specimens. The results are shown in Fig. 3. We find that comparing with the 2# specimen, the 1# specimen has a relatively higher FWHM value, which means that more FCT phases forms in the Mn–Cu–Al samples. However, from 128 to 256 h, there is a sharp decrease in FWHM for both of the specimens, suggesting that the FCT phases decrease as the holding time is more than 128 h.

3.3 *IF* measurement

To determine the effect of thermal relaxation behavior on the damping capacity, we measured the room-temperature IF of the $1^{\#}$ and $2^{\#}$ specimens after holding at 120℃ for 16, 128, 256, 512 h, respectively. The IF values corresponding to the strain amplitude of 800×10^{-6} are shown in Fig. 4. One can see that for the specimens, there is a sharp damping decrease within the same holding time between 128 and 256 h, although the damping capacity is stable in the initial 128 h for the $2^{\#}$ specimen and even increases as high as 13.7% for the $1^{\#}$ specimen. Considering the FWHM performance in the same period in Fig. 3, we believe that the relaxation behavior of Mn-rich FCC phases happens from 128 to 256 h. As a result, the FCC–FCT transition is affected and hence fewer FCT phases form in matrix. To further describe the relaxation performance, we fit the experimental data by taking the function (1) in Sect. 2.2. The corresponding parameters are given in Table 2. It reveals that the τ value of the $2^{\#}$ specimen is a little larger than that of the $1^{\#}$ specimen. Thus, the addition of Fe decreases the relaxation tendency of the FCC phases in the alloys.

3.4 Microstructural observation

For the $1^{\#}$ and $2^{\#}$ specimens held for 512 h, we observed their textures by SEM. The BSE photographs are shown in Fig. 5a and b. From these figures, many precipitates appear in the specimens. Moreover, comparing with the $1^{\#}$ specimen, the $2^{\#}$ specimen has more precipitates either in the crystals or at grain boundaries.

Figure 6 shows the TEM photographs of precipitates distributing along the grain boundaries in the specimens. According to the selected area electron diffraction (SEAD) pattern (Fig. 6a) and their EDS spectra (Fig. 6b), it can be confirmed that the precipitates are *α-Mn* particles, which was mentioned before in Reference [9].

Under TEM, we also observe many intragranular precipitates in the $2^{\#}$ specimen. Figure 7a shows their TEM image and SEAD pattern. It shows that the precipitates distribute in crystal in chains. According to their SEAD patterns, the particles are BCC structure and their lattice parameter is 2.8737 Å. From the EDS (energy dispersive X-ray spectroscopy) spectra in Fig. 7b, the particles contain 61.85 wt% Fe, 33.621 wt% Mn, and 0.630 wt% Cu. Thus, the precipitations are FeMn phases. In particular, we still observe some streakings in diffraction pattern in Fig. 7a. It reveals that there are dislocations in these crystals.

4 Discussion and conclusion

The thermotolerance is very important for the Mn–Cu alloys as the application temperature occasionally exceeds the phase transition temperature A_s. However, point defects (Zener relaxation) may lead to the thermally activated relaxation as the ambient temperature is higher than 100℃. In recent years, some researches confirm that the Mn-rich FCC phases in Mn–Cu alloys relax after holding at a higher temperature for a long time [2, 3]. In our experiments, because the heating temperature of 120℃ is higher than the A_s temperatures of the $1^{\#}$ and $2^{\#}$ specimens (92.4 °C and 44.2 °C, respectively), nearly all of the FCT phases transform into FCC phases in the thermal process. As the heating time is extended, more and more vacancies move to the dislocations and boundaries of FCC phases, causing the relaxation of matrix. Nevertheless, the *IF* value distinctly drops from 128 to 256 h. Our XRD results in Sect. 3.2 reveal that the number of FCT phases in the alloys decreases as the holding time is more than 128 h. Thus, we suppose that the excessive heat-induced relaxation increases the stability of the Mn-rich FCC phases, actually weakening the transition kinetics from FCC to FCT.

As an alloying composition, many researchers believe the Fe element enhances the FCC phase stability. Sakaguchi et. al. have confirmed the role of Fe in a MnCuNiFe alloy [7]. Our research also shows that in comparison with the $1^{\#}$ alloy, the $2^{\#}$ alloy has the lower transition temperatures of A_s and M_s. In our opinion, the FeMn particles (See Fig. 5 and 7) decrease the Mn content of around areas. Hence, the *IF* value of the $2^{\#}$ alloy is lower than that of the $1^{\#}$ alloy. However, the relaxation parameter τ of the $2^{\#}$ alloy is a relatively higher than the $2^{\#}$ alloy (see Table 2). It means that the addition of Fe restrains the excessive relaxation performance of the Mn-rich FCC phases above the A_s temperature.

Acknowledgements This study was funded by National Natural Science Foundation of China (No. 11172248) and Natural Science Foundation of Jiangsu Province.

Compliance with ethical standards

Conflict of interest The author(s) declare that they have no competing interests

References

1. Deng C, Peng W, Xiong Z et al (2020) Spinodal decomposition and martensitic transformation kinetics of the 82.2Mn-15.8Cu-2Al thermosensitive damping alloy. Thermochimi Acta 683:178321
2. Fukuhara M, Yin F, Ohsawa Y et al (2006) High-damping properties of Mn–Cu sintered alloys. Mater Sci Eng, A 442:439–443
3. Hou S, Qin F, Han J et al (2018) Strain glass transition in high damping Mn-22Cu-5Ni-2Fe alloy. Prog Nat Sci: Mater Int 28:614–617
4. Laddha S, Aken DV, Lin H (1997) The effect of carbon on the loss of room-temperature damping capacity in copper-manganese alloys. Metall Mater Trans A 28:105–112
5. Liu C, Yuan F, Gen Z et al (2016) In-situ study of surface relief due to cubic-tetragonal martensitic transformation in Mn69.4Fe26.0Cu4.6 antiferromagnetic shape memory alloy. J Magn Magn Mater 407:1–7
6. Markova GV (2004) Internal friction during martensitic transformation in high manganese Mn–Cu alloys. Mater Sci Eng, A 370:473–476
7. Sakaguchi T, Yin F (2006) Holding temperature dependent variation of damping capacity in a MnCuNiFe damping alloy. Scripta Mater 54:241–246
8. Sun LY, Vasin RN, Islamov AK et al (2020) Influence of spinodal decomposition on structure and thermoelastic martensitic transition in MnCuAlNi alloy. Mater Lett 275:128069
9. Vitek JM, Warlimont H (2013) On a metastable miscibility gap in γ-Mn-Cu alloys and the origin of their high damping capacity. Met Sci 10:7–13